TABLE 6

Pressure cells used in Raman spectroscopy

Type of cell	Optical instrument	Pressure limits (kbar)	Temp. limits (K)	Windows	Remarks	Ref.
Opposed anvil	Spex 1401	100	77—350	Diamond	Solids	59
Drickamer	Spex 1401	100	77—350	Diamond	Solids	45
Opposed anvil	Spex 1401 Cary 81	200	573	Diamond	Solids, liquids	60, 61
Hydrostatic gas pressure	Spex 1401	9	77—290	Sapphire, quartz	Solids, gases	38
Waspaloy (opposed anvil)	Spex 1401	200	to 973	Diamond	Solids, liquids, solutions	54
Drickamer	Spex 1400	100	4—1300	NaCl, diamond	Solids, liquids solutions	46
Daniels	Spex 1400	10	R.T.	Sapphire	Solids	79
Sapphire, back-scattering	Cary 81	11	473—573	Sapphire	Solutions, solids, liquids	80, 81
Piston-cylinder	Jarrell-Ash	< 3		Sapphire	Solutions, liquids	82
Piston-cylinder	Coderg	10	2—300	Sapphire	Solids, liquids, solutions, gases	83
Opposed anvil	Coderg	30		Diamond, sapphire	Solids	53, 74
Daniels	Spex 1401	10	77—400	Sapphire	Solids, liquids, and Brillouin spectra	84—86
Piston-cylinder	Spex 1401	7	1.4 to R.T.	Sapphire	Solids	87
Pressure vessel	Jarrell-Ash	220	100—700	Diamond	Solids, liquids, solutions	88
Special cell	Spex 1405	3	223—473	Quartz	Liquids, gases	89
Drickamer	Cary 81	55	77—500	Sapphire	Solids	a

[a] Personal communication with W.F. Sherman, Physics Department, King's College, University of London, Strand, London WC2R 2L5, Gt. Britain.

TABLE 7

High pressure in optical materials [a]

Material	Spectral range (μm)	Refractive index [b] at λ (μm)	Modulus of rupture [b] (p.s.i.)	Young's modulus [b] (p.s.i.)	Compressive strength (p.s.i.)	Hardness Knoop No.	Solubility (g/100 g H_2O)
NaCl	0.2—15	1.52 at 4 1.4 at 10		5.8×10^6		15.2—18.2	35.7(0°C)
Lithium fluoride, LiF	0.11—6	1.35 at 4 1.1 at 10		$9.40—11 \times 10^6$		102—113	0.27(18°C)
Irtran 1, MgF_2	1—8	1.35 at 4	21 800	16.6×10^6	157 600	576	0.0076 (18°C)
Calcium fluoride, CaF_2	0.13—9	1.41 at 4		$11—15 \times 10^6$		158	0.0016 (18°C)
Irtran 3, CaF_2	1—10	1.41 at 4 1.34 at 8.3	5 300	14.3×10^6		200	Insoluble
Irtran 2, ZnS	2—14	2.25 at 4 2.20 at 10	14 100	14×10^6	121 200	354	0.00069 (18°C)
Irtran 4, ZnSe	0.5—20	2.5 at 4 2.4 at 10	6 100	10.3×10^6		150	Insoluble
Magnesium oxide, MgO	≤6.8	1.7 at 2.2 1.66 at 4.3		3.6×10^6		690—692	0.000012
Irtran 5, MgO	1—8	1.67 at 4 1.60 at 6	19 200	48.2×10^6		640	0.00062

Sapphire, Al_2O_3	$\leqslant 5.5$	1.73 at 2.2	50.56×10^6	1370 1525—2000	9.8×10^{-5}
Diamond *	c				
Type I	2—4, 5.5—7, 10—16	2.4173		7000	Insoluble
Type II	0.26—4; 5.5 through FIR				
Ceramic barium titanate, $BaTiO_3$	$\leqslant 6.9$	2.4 at 2.2, 4.3	16.50×10^6		
Calcite, $CaCO_3$	0.2—5.5	$\cong 1.7$			
Germanium	1.8—2.3	$\cong 4.0$			
Silicon	1—9	3.43 3.42			
Fused silica SiO_2 (Corning 7905, GE type 101-100, Infrasil)	0.3—3.5	1.43			
NBS F158 SiO_2	4.5	1.80			
Bausch & Lomb d					
RIR-2	4.5	1.75			
RIR-10, 11, 12	5.0	1.62			
RIR-20	5.5	1.82			

* Diamond has the highest Debye temperature and type II diamonds demonstrate higher thermal conductivity than type I diamonds (see C.Y. Ho, R.W. Powell and P.E. Lilly, J. Phys. Chem. Ref. Data, Supp. 1, 3 (1974) L-118. [a] Taken in part from ref. 72. [b] 298 K. [c] UV and visible absorption and FIR depend upon particular type of diamonds used here. [d] Calcium aluminate ($CaO—Al_2O_3$) and similar materials. [e] Note that UV limitations exist for all of these materials in addition to those of diamonds.

with both diamonds. An improved method for coupling the DAC optically with a Raman spectrometer has been discussed by Adams et al. [74]. The fluorescence problem of diamonds under laser excitation and its effects on the Raman measurements in a DAC are discussed by Adams and co-workers [53,72,75].

The first high pressure Raman study with a piston-cylinder cell was made by Gonikberg and co-workers [76]. A Raman study using a piston-cylinder cell (Daniel type) which gives hydrostatic pressure has been made [77—79]. Figure 7 illustrates this cell. Walrafen used a back-scattering Raman cell equipped with windows made of single crystals of sapphire [80]. Nicol et al. [46] and Ferraro [45] have used the Drickamer cell for Raman studies.

Table 6 summarizes the various pressure cells used for Raman spectroscopy at high pressures.

(iv) Optical windows for use at high pressures

For the anvil-type high pressure cells the window material serves the dual purpose of transmitting the pressure and being transparent to the electromagnetic radiation of interest. In the Drickamer piston-cylinder cell this is also true in part, although the mechanism of pressure transmission is not done by the window. Table 7 lists a number of possible windows for use at high
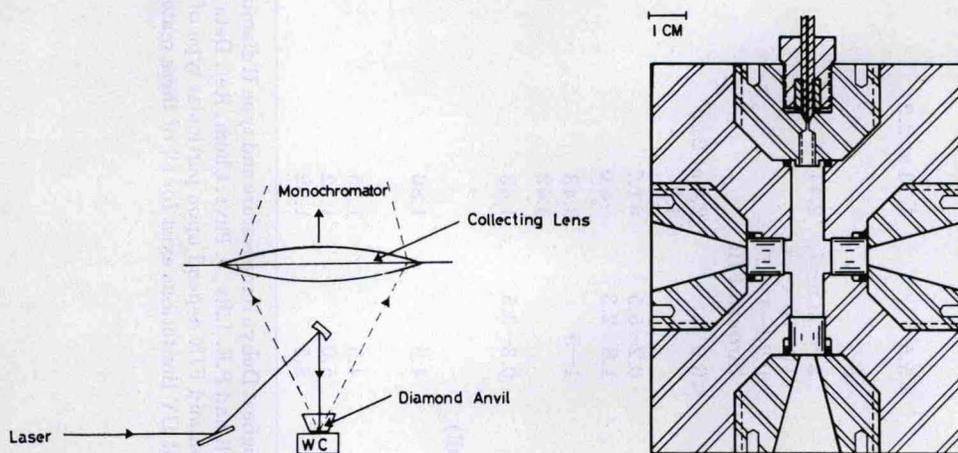
Fig. 6. Details of DAC with one tungsten carbide anvil [53]. (Figure reproduced through the courtesy of the authors and Applied Spectroscopy.)

Fig. 7. Daniels-type Raman cell [77—79]. High pressure optical cell with three oriented single crystal synthetic sapphire windows. The C axes of the sapphire windows are oriented normal to the flat window faces. (Figure reproduced through the courtesy of the authors and Review of Scientific Instruments.)

pressures. The diamond window is by far the most valuable for high pressure studies. It is the hardest material known and is transmissive throughout most of the electromagnetic regions. Generally, two types of diamonds are used — type I and type II. However, there may be variations from diamond to diamond, as has been indicated [53,72,75]. Type I shows absorption at ca. 3, ca. 4—5.5, ca. 7—10 μm while type II absorbs at ca. 3 and ca. 4—5.5 μm. Sapphires may be used in the IR region from 2—5 μm, although pressures are limited to about 12 kbar. Sapphire is promising for Raman pressure studies, since it may be used from $\Delta\nu$ of 500—2000 cm^{-1}, before fluorescence becomes a problem. However, pressure limits are low with sapphire windows.

Other measurements have been made with pressure, but these are beyond the scope of this review. For example, electrical conductivities [55,90,91], magnetic susceptibilities [92—100], the Mössbauer effect [101—104], magnetic resonance [105—113], nuclear quadrupole resonance [114—117], X-ray [118—124], and viscosity [125] have all been studied under pressure. However not all these studies have been made with the DAC.

C. PRESSURE CALIBRATION

It has been mentioned that a pressure gradient exists in the DAC. Duecker and Lippincott [58] have demonstrated that the pressure gradient face is parabolic, with pressures in the center reaching 1—1/2 times those on the edges. Any pressure in the contact area of the diamond is in reality only an average pressure, unless a gasket and a pressure-transmitting fluid is used.

Calibration of the DAC and for that matter other anvil-type cells can be made by several methods. Unfortunately, a number of these methods involve internal calibration incorporating a foreign substance, and the problem of a matrix effect is omnipresent. The methods are listed as follows: (1) The compression of the spring is measured by a Dillon force gauge. The contact area of the diamond is determined by means of microphotographs. One can thus obtain force per unit area of pressure. (2) Solids which undergo phase transitions at known pressure may be used to calibrate the cells. For example, KBr shows a phase transition at 18 kbar; KCl at 20 kbar; $NaNO_2$ at 14 kbar; HgI_2 at 13 kbar. These phase transformations can be followed with pressure using a microscope as well as being followed spectroscopically. (3) Calibration may be made by following the change in nickel dimethylglyoxime (NDMG) in the visible absorption region [58,126]. These changes have been related to pressures by the National Bureau of Standards. However, NDMG tends to lose intensity with pressure and the band being monitored is eventually too weak to follow. Other nickel complexes have been suggested [127,128]. (4) Scientists at the National Bureau of Standards [54,55,129—131] suggested calibration of the DAC by following the R_1R_2 doublet fluorescence lines at 694.2 and 692.8 nm with a pressure increase. Figure 8 shows the pressure calibration of the ruby R_1 fluorescence line. The freezing points of several liquids (e.g., CCl_4, H_2O, n-C_7H_{16}, and C_2H_5Br) and two solids, which have character-

RUBY R$_1$ FREQUENCY SHIFT − $\Delta\bar{\nu}$ (cm^{-1})
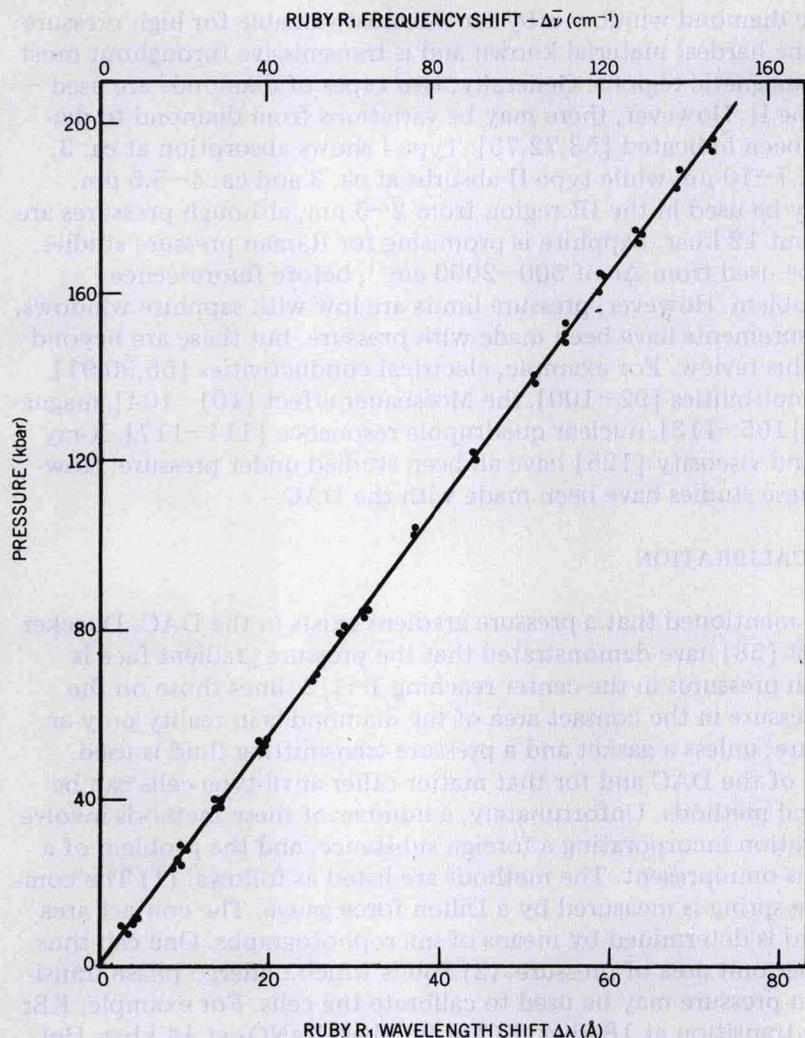
Fig. 8. Pressure calibration of ruby R_1 fluorescence line to ca. 160 kbar [55,129—131]. (Figure reproduced through the courtesy of the authors and the American Institute of Physics, New York.)

ized pressure transitions, were used in establishing the pressure response with cm^{-1}. It was suggested that the method can be used to high pressures (mbar region) since no significant departure from linearity in the curve occurs, and further that the method is useful to ca. 973 K.

The use of the ruby R_1 fluorescence line as a function of pressure has now been extended into the megabar region [90,132—135]. This was done by simultaneously measuring the specific volume of Cu, Mo, Ag and Pb, and

referring the results to isothermal equations of state derived from shock-wave experiments.

The piston-cylinder type cells have been calibrated by measuring bismuth and barium transition pressures or the resistance changes with pressure of various metals (e.g., manganese, lead, iron, barium, calcium and rubidium) [33]. In some cases, pressure transducers are used to measure the pressures [136]. Alternatively, the NDMG or ruby methods, crystals showing phase changes, or a change in the index of refraction may be used. For reviews on pressure calibration see refs. 17 and 137.

D. CHOICE OF OPTICAL REGIONS TO USE AS A PROBE

The optical region one chooses for pressure studies depends on the particular application. For ionic or pseudo-ionic crystals the far IR region (FIR) is the most useful, since all of the lattice modes occur in this region. For organic compounds the "fingerprint" (mid-IR) region is the most useful. For coordination compounds of the MX_n type, where X = halogen, pseudo-halogen or inorganic anion, the low frequency region is useful as the metal—X vibrations are located there. However, the visible region should be examined conjunctively to monitor the "$d-d$" transitions. For coordination compounds involving organic ligands (of the type ML_nX_m where L = organic ligand) the FIR may offer some complications since the organic ligands' strong absorptions could mask the M—X or M—L vibrations. In that case, the visible region may be used. If L = CO or en, one can resort to the mid-IR region using sapphire windows (ν_{CO} in 5 μm range), since diamond has absorption in this region. If L = NO one may use the mid-IR region likewise, but in this case one must use diamond windows (ν_{NO} in the range 6—6.5 μm), since sapphire shows absorption in this region. For heavy element complexes such as the actinide or lanthanide complexes, the FIR is perhaps the most useful, as "$f-f$" transitions appear to be less pressure-sensitive than "$d-d$" transitions [138]. Whenever possible, it would be better to use several optical probes to study a particular pressure change.

E. VIBRATIONAL STUDIES AT HIGH PRESSURES

The opportunity to subject a molecule to an external perturbation such as pressure and measure the resultant changes by spectroscopic techniques, affords the scientist an additional mechanism whereby he can study physical and/or chemical changes. Vibrational spectroscopy becomes a viable method of studying these changes, for in most cases the space group is changed and this is reflected by changes in the vibrational selection rules.

The area of vibrational spectroscopy of molecules subjected to pressure was long neglected [139]. The reasons for the neglect were probably experimental since it was easier to cool or heat a material, and these non-ambient temperature experiments did not require microtechniques in IR or Raman that are

required with pressure measurements. The strides that the matrix isolation technique has made in the past 10 years attests to this. However, the advent of the DAC in 1959 [48] generated the notion that vibrational spectroscopic techniques used conjunctively with pressure were possible. This paper is planned to present a review of the accomplishments of the past 20 or so years, since Weir and co-workers constructed the DAC [48]. In most cases the review will concern itself with results obtained with the DAC.

(i) Inorganic compounds

Primary motivations in studying solid inorganic systems have been based on studying pressure effects on various polymorphs, those stable under ambient conditions and those achieved only under high pressures. In this way phase diagrams, previously unknown, can be constructed or adjusted. In cases where no X-ray is known (e.g., phases obtainable only at elevated conditions of temperature and pressure) some inference may be obtained on the nature of the space group involved from the spectroscopic results. In certain instances interest has been based on obtaining order-disorder information existing in the various phases of a material (for example, electrical conducting phases). Comparisons of intra- and intermolecular forces, the latter being pressure sensitive, are also of interest. Of interest are hydrogen bonded systems where pressure shows effects which can be observed by studying the vibrational spectra.

(1) Mercuric halides

Adams and Appleby [140] have investigated the halides of Hg(II) under high pressure. The three phases (I, II and IV), of $HgCl_2$ have been subjected to pressures up to 30 kbar. Results are shown in Table 8. The Raman and IR spectra of phases I and IV were found to be similar, and it was concluded that a second-order transition characterized by molecular orientation with retention of the space group was involved. Phase II was found to be entirely different and to approximate a T_h^6 structure with $z = 4$, based on the spectroscopic results. Phases I and IV possess a D_{2h}^{16} space group with $z = 4$.

All four phases of $HgBr_2$ (I, II, III and IV) were investigated by Raman and IR techniques to 50 kbar [141]. Phases I and II were considered to have similar structures. Phase III appears to possess a C_{2h} space group, and phase IV probably has a CdI_2 structure. These conclusions were reached, based on the spectroscopic results obtained. Table 9 tabulates the Raman frequencies at various pressures.

Early superficial Raman experiments with HgI_2 have been made [59,60]. In a more thorough study the high temperature (127°C) phase and the high pressure phase (ca. 13 kbar) of HgI_2 were compared, using Raman and far IR data [142]. The red, ambient temperature, HgI_2 has a $P4_2/nmc$ (D_{4h}^{15}) space group, $z = 2$, with 4 iodine atoms around the mercury atom [143]. At 127°C it turns yellow and this phase has a $Cmc2_1$ space group with $z = 4$ [144]. At

TABLE 8

Raman and IR results for phases I, IV and II in the $HgCl_2$ system [140]

Phase	Raman (cm^{-1})	IR (cm^{-1})
I (Ambient pressure)	383 (vvw)	370 (vs)
	315 (s, sp)	330 (vw)
	167 (vvw)	310 (w)
	126 (w)	100 (vs)
	74 (m)	75 (sh)
	43 (vw)	
	23 (m)	
	18 (s)	
IV (8.5 kbar)	386 (vvw)	370 (vs)
	316 (s, sp)	330 (w)
	170 (vvw)	310 (w)
	144 (w)	100 (vs)
	133 (w)	77 (sh)
	77 (m)	
	51 (w, sh)	
	41 (vvw)	
	21 (m)	
II (30 kbar)	312 (vs)	369 (vs)
	178 (s)	100 (vs)
		72 (vs)

13 kbar red HgI_2 converts to a yellow phase. Differences are observed in both the IR and Raman spectra of the two yellow phases. The high pressure phase has a more complex far IR spectrum than the high temperature phase, especially in the 80 cm^{-1} region. In the Raman spectrum the 145 cm^{-1} band in the high pressure phase has a shoulder, which is missing in the low temperature

TABLE 9

Raman frequencies (cm^{-1}) for $HgBr_2$ at various pressures (R.T.) [141]

	Pressure (kbar)						
	0	6.3	18.8	23.3	31.6	35.7	49.5
Phase	I	II	II	III	III	IV	IV
				191	191		
	186	185	184	184	184	179	176
				74	77	78.5	77
	57	61	60	60	69		
				50	49		
	40	38					
	17.5	22	24				
	15	17	18				

phase. The low temperature phase has Raman bands at 15 and 11.5 cm^{-1}, which are missing in the pressure phase. Although the high pressure phase of HgI_2 remains unknown, the vibrational spectrum resembles that of phase III of $HgBr_2$, and would thus appear to have a structure with a higher coordination number, consistent with consequences of increased pressure.

Studies of the effect of pressure on the ν_{HgCl} vibration in $HgCl_2 \cdot$ dioxane have been made [145]. This vibration shifts 18 cm^{-1} towards lower energy, while modes of the organic ligand bands at 854, 614 and 290 cm^{-1} are raised by ca. 5 cm^{-1}.

(2) Alkali metal cyanides

The various polymorphic phases of KCN and NaCN have been investigated using vibrational spectroscopy at high pressures [146]. Table 10 lists structural data for the polymorphs of KCN and NaCN. Raman frequencies are listed in Table 11 for KCN polymorphs at various pressures. The behavior of the cyanide vibration with pressure in KCN and NaCN is shown in Table 12. The Raman scattering of $K[Ag(CN)_2]$ has recently been measured to 18 kbar [146a]. Two high-pressure polymorphs were identified. A dramatic change in the pressure dependency of the CN stretching vibration was noted. The pressure of other internal and external modes was also determined.

(3) Nitrates, carbonates

Infrared spectra of KNO_3 have been obtained at pressures up to 40 kbar [147]. The pressure range of KNO_3 (III) with a symmetry $R3m$ (C_{3v}^5) with $z = 1$, is very narrow and at 4 kbar and 38°C converts to KNO_3 (IV). For this phase a new band was observed at 717 cm^{-1}. The 825 cm^{-1} absorption shifts to 831 cm^{-1} and increases in intensity with pressure. ν_3 and ν_1 show a small shift to higher frequency, and a slight increase in intensity. The various combinations involving the NO_3^- vibration lose intensity with pressure. It was observed that ν_1 is more sensitive to pressure than ν_4, and ν_2 is insensitive. The

TABLE 10

Structural data for the NaCN and KCN polymorphs [146]

Phase		Structure	Z
KCN	I	Cubic, $F_{m3m}(O_h^5)$	4
	III	Cubic, $P_{m3m}(O_h^1)$	1
	IV	Monoclinic, $Cm(C_s^3)$	2
	V	Orthorhombic, $I_{mmm}(D_{2h}^{25})$	2
	VI	Orthorhombic, $P_{mmn}(D_{2h}^{13})$	2
NaCN	I	Isostructural with KCN I	
	II	Isostructural with KCN V	
	III	Isostructural with KCN VI	

TABLE 11

Raman frequencies (cm^{-1}) for KCN polymorphs [146]

Pressure (kbar)	0.001	6.58	16.5	20.1	27.6	0.001	0.001	21.7
Temp. (K)	293					87	60	383
Phase	I	I	I	I & IV	IV	V	VI	III
ν_{CN}	2078.2 [a]	2083.5	2090	2090 2088 (sh)	2090	2080.0 [a]	2081.1 [a]	2090

[a] $\pm$ 0.2 cm^{-1}; all others $\pm$ 0.5 cm^{-1}.

24

TABLE 12

ν_{CN}	$d\nu/dp$ $(cm^{-1}\ kbar^{-1})$ [146]
KCN I	0.50 (20°C)
KCN I	0.574 (110°C)
KCN III	0.45 (110°C)
KCN IV	0.32 (20°C)
NaCN II	0.57

results are consistent with a unit cell of high occupancy and low symmetry.

$AgNO_3$ has also been investigated at high pressure [148]. Adams and Sharma [148] have studied phases I, II, III and metastable phase V. In the latter phase doublets occur in ν_4, ν_1 and $(\nu_1 + \nu_4)$ regions, and with the shape of the ν_3 envelope are all indicative of a low site symmetry and relatively high unit cell occupancy.

The first solid studied in the DAC was calcite, $CaCO_3$ [149]. The results showed that ν_1, normally IR inactive, appeared in the spectrum with pressure; ν_2 shifted from 882 to 865 cm^{-1} and splitting of ν_4 occurred. Other studies were made with calcite up to 61 kbar. The authors pointed out that the spectra at higher pressures resembled that of a calcium carbonate polymorph, vaterite, with a hexagonal unit cell containing 2 or more molecules per unit cell. Fong and Nicol [150] have studied $CaCO_3$ to 40 kbar, and have interpreted their data in terms of two phases of calcite, II and III, occurring at 14 kbar and 18 kbar. Recent Raman spectra have verified that the high pressure phases are not aragonite [151]. Only superficial studies have been made with aragonite and $MgCO_3$ under pressure [48].

(4) NaNO$_2$ and KNO$_2$

Infrared spectra of KNO_2 and $NaNO_2$ and Raman spectra of the polymorphs of KNO_2 have been studied at high pressures [152,153]. $NaNO_2$ (C_{2v}^{20}, $z = 1$) undergoes a phase transition at 39°C and 10 kbar and KNO_2 undergoes a transition at 6.3 kbar. In the IR studies it was determined that the symmetric modes lose intensity with pressure and all bands undergo blue shifts. The Raman studies have led to conclusions concerning the nature of the polymorphs and the order-disorder in these phases.

(5) Dihydrogen phosphates

The paraelectric crystals of KH_2PO_4 and RbH_2PO_4 were studied by IR at pressures to 60 kbar [154]. For both compounds the protons were found to be dynamically disordered between the two possible O·H···O sites connecting the PO_4^{3-} groups. A new phase was found at 10 kbar in which the hydrogens became ordered while the PO_4^{3-} tetrahedra became disordered. In pressure

studies of KH_2PO_4 to 9.3 kbar a soft mode in the crystal became under-damped with the application of pressure [155]. Studies with RbH_2PO_4 were made at 21 kbar using Raman spectra as the optical probe [156]. These results indicated a large decrease in transition temperature with pressure and a disappearance of the ferroelectric state at all temperatures for $p \geqslant 15.2$ kbar, and a decrease with pressure of the Curie constant and dielectric constant in the paraelectric phase.

(6) Molybdates, tungstates, sulfates

The Raman spectra of $CaMoO_4$ and $CaWO_4$ have been obtained at pressures to 40 kbar [157]. A new pressure phase for each compound was found. The pressure dependencies of the internal modes for these compounds were determined and found to range from 0.0 to 1.0 cm^{-1} $kbar^{-1}$.

Some sulfates were superficially examined at high pressures [64]. ν_4 of SO_4^{2-} anion showed shifts of 3 cm^{-1} at 35 kbar, while a lattice mode at 183 cm^{-1} showed a blue shift of 52 cm^{-1}.

(7) Bihalide salts

The bihalide salts of $NaHF_2$, KHF_2, NH_4HF_2, $(CH_3)_4NHCl_2$ and $(C_2H_5)_4NHCl_2$ were investigated by IR techniques at pressures up to 40 kbar [158]. In these strong hydrogen bonded systems the ν_3 vibration in the HX_2^- anion shifts to higher frequencies while the ν_2 vibration shifts to lower energies with an increase in pressure. The ν_1 frequency was deduced from the behavior of combination bands and found to shift toward higher frequencies. These results are typical expectations for a simple model of strong hydrogen bonding. A new phase of $NaHF_2$ was found at 40 kbar.

(8) Ionic conductors

The pressure dependent Raman spectra of the fast ion conductors β-Ag_2HgI_4 and β-Cu_2HgI_4 were measured [159]. The Raman spectra of β-Cu_2HgI_4 ($I42m$ (D_{2d}^{11}), $z = 2$) was followed at 25°C to 24 kbar, and no phase transition was observed. The breathing motion of the iodide lattice against the Cu^{2+} ions at 85 cm^{-1} undergoes a more rapid blue shift than the Hg—I stretch at 127 cm^{-1}, indicative of greater anharmonicity in the CuI_4 stretching mode as compared to the HgI_4 stretch. The 36 cm^{-1} mode shows a negative pressure dependence.

β-Ag_2HgI_4 (I_4^- (S_4^2), $z = 2$) shows several phase changes in the 0—10 kbar region. Table 13 shows band positions in Ag_2HgI_4 at various pressures and at 60°C. At 6.1 kbar and 25°C, the HgI stretching vibration lowers from 124 to 116 cm^{-1} and may indicate a change from 4-coordinate to a 6-coordinate environment. Figure 9 shows the Raman spectra of β-Ag_2HgI_4 as a function of pressure. A second phase is observed between 7.5—44 kbar and another phase at pressures greater than 44 kbar.

The Raman spectra of these materials have been found useful in screening potential ionic conductors [160,161]. Broad Raman bands are indicative of

...ycrystalline Ag_2HgI_4 at various pressures [a] [159]

Position (cm^{-1})						
	24.2 (s)	29.5 (w)		34.9 (s)	80 (w, br)	
	23.8	—		35.1	—	
19.1 (s)			32.8 (w)			
19.3			34.2			
17 (s, br)			123 (s, br)		~142 (m, sh)	
	29 (m)	114 (vs)				

[a] anvil cell with paraffin oil as a pressure transmitting liquid was used.
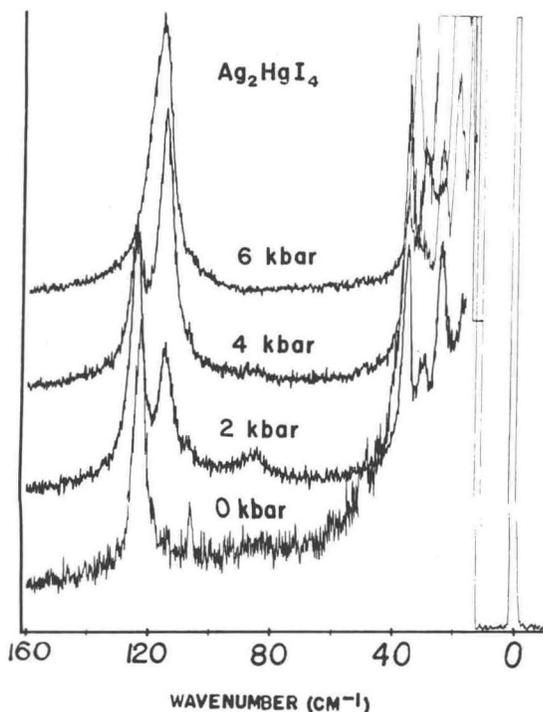
Fig. 9. Raman spectra of β-Ag$_2$HgI$_4$ as a function of pressure [159]. (Figure reproduced through the courtesy of the authors and the American Institute of Physics, New York.)

ionic conductors and disorder. The sudden sharpening of the bands at 6.1 kbar is an indication of electronic conduction and a more highly ordered structure. The results are used to determine the anharmonicity in superionic conductors [159]. Both CuI and HgI modes are highly anharmonic, and a highly anharmonic potential may be important in providing a low energy barrier for ion motion and ionic conductivity.

(9) Miscellaneous inorganic compounds

(a) Ammonium halides. Wong and Whalley [162] have made a Raman study of NH$_4$F and Ebisuzaki and Nicol [163] have examined NH$_4$Cl under pressure using Raman spectroscopy. At 10 kbar a disordered-ordered phase transition takes place in NH$_4$Cl. The lattice mode involving movement of the NH$_4^+$ and Cl$^-$ sublattices shows a pressure dependency of 2.65 cm^{-1} kbar^{-1} in the disordered (low pressure) phase. The librational mode behaves similarly. With the exception of the ν_2 bending vibration in NH$_4^+$ the internal modes all show negative pressure dependencies varying from -0.1 to -1.2 cm^{-1} kbar^{-1} and are attributed to the increased hydrogen bonding occurring in the ordered high pressure phase.

(b) Solid nitrogen. The Raman spectra of the three known phases of solid nitrogen at high pressures (0—10 kbar) and low temperature (8—220 K) were obtained [164]. The high pressure γ phase is tetragonal with D_{4h}^{14} space group and $z = 2$. The observed frequencies and relative integrated intensities were determined. Table 14 tabulates results at various temperatures. By comparing the results with calculated frequencies and relative intensities the low- and high-frequency bands in the lattice region were assigned as librational modes, E_g and B_{1g}, respectively.

(c) Water ice. In passing I wish to cite the work of Whalley and co-workers on water ices. The IR spectra of water ice II, III, V, VI and VII at appropriate pressures and temperatures were measured [165]. The Raman spectra for ices I_h, I_c, II, III and V were also obtained by Marckmann and Whalley [166].

(ii) Ionic and pseudo ionic crystals with lattice vibrations

Considerable interest has developed in examining the pressure dependence of vibrational lattice modes in neat, ionic and pseudo ionic, and mixed crystals. The interest in pressure studies stems from results which can be obtained that can be used for testing lattice dynamics theory. Results are generally reported in terms of a Grüneisen parameter. Both temperature and pressure data provide information on anharmonic contributions to the lattice frequency shift. The temperature dependence of the peak position and half-width of lattice modes consist of the purely volume dependent part of the Grüneisen equation of state and the anharmonic contributions. On the other hand, the pressure dependence of peak position arises chiefly from the volume dependent part of the Grüneisen equation. Comparison of the Grüneisen parameter obtained from both methods can provide some estimate of anharmonicity existing in these solids.

TABLE 14

Observed Raman frequencies and relative intensities for the γ-phase of solid N_2 [164]

Temp. (K)	$\nu(\text{cm}^{-1})$	Relative integrated intensity
35	57.5	2
	95.5	4.5
	2329	1
20	58.2	5.5
	102.5	3
	2330	1
8	58.4	7
	103.6	2.5
	2331	1